Prethermalization in the cooling dynamics of an impurity in a Bose-Einstein condensate

Tobias Lausch, Artur Widera, and Michael Fleischhauer*
Department of Physics and State Research Center OPTIMAS, University of Kaiserslautern, 67663 Kaiserslautern, Germany

(Received 13 October 2017; published 13 February 2018)

We discuss the cooling dynamics of heavy impurity atoms in a Bose-Einstein condensate (BEC) by emission of Cherenkov phonons from scattering with the condensate. In a weakly interacting low-temperature condensate, different scattering processes result in a separation of time scales of the thermalization dynamics. Prethermalized states are formed with distinct regions of impurity momenta determined by the mass ratio of impurity and BEC atoms. This can be employed to detect the mass renormalization of the impurity upon the formation of a polaron and paves the way to preparing nonequilibrium impurity-momentum distributions.

DOI: 10.1103/PhysRevA.97.023621

I. INTRODUCTION

Cooling atomic quantum gases down to ultralow temperatures has opened a window to experimental exploration of quantum phenomena [1–3]. Beyond probing of ground-state properties of quantum objects, quantum gases offer the possibility to induce and study nonequilibrium and relaxation dynamics. Tight control over trapping potentials has allowed shedding light onto the nonequilibrium dynamics of integrable systems, which, owing to the large number of conserved quantities, can stay at a nonthermal steady state [4,5], described by a generalized Gibbs ensemble [6]. Weak integrability-breaking perturbations will eventually lead to thermalization, but a separation of time scales can give rise to long-lived prethermalized states [7,8]. While much attention is paid to nearly integrable quantum systems, also the thermalization dynamics of nonintegrable systems can be nontrivial including long-lived prethermalized states resulting from dynamical constraints. Understanding here the microscopic details will help elucidate open questions of quantum thermalization. A powerful tool to trace this microscopic thermalization dynamics is the immersion of impurities in a quantum gas [9–12]. In particular, for the paradigmatic system of single impurities in a Bose-Einstein condensate (BEC), the momentum-dependent transition to superfluid dynamics is expected to have a profound impact on the thermalization. In the present paper we show that, even though the system is nonintegrable, this can lead to a separation of time scales between a fast relaxation into a prethermalized state and the eventual approach of thermal equilibrium. Moreover, when the impurity is decelerated below the critical momentum of superfluidity, polaronic quasiparticles form [13–19], which has been observed recently for strong coupling [20,21]. The polaronic modifications of the quantum state can alter the prethermalized state. This may allow access to properties of these quasiparticles such as the polaronic mass renormalization for small modifications.

In this article we provide a microscopic description of the cooling dynamics of a single mobile impurity immersed in a three-dimensional (3D) BEC [see Fig. 1(a)] using a simple perturbative Boltzmann equation. Assuming only energy and momentum conservation, we find that for impurity momenta larger than the Landau critical momentum p_c, deceleration and cooling of the impurity are achieved by Cherenkov-type emission and scattering of Bogoliubov excitations, a mechanism previously suggested in Refs. [22–24] and explored experimentally in Refs. [25,26]. In contrast to these earlier works, we consider theoretically a scenario not involving lattice potentials and which is experimentally easily implementable [27]. Furthermore, we find that in leading order of the impurity-BEC interaction and for impurity masses larger than the boson mass, additional critical momentum regions emerge characterized by lower cutoff momenta [$p_c^{(1)}$ in Fig. 1(b)], which we interpret as a consequence of the superfluid nature of the bath. For a weakly interacting BEC, scattering processes into and out of these regions will occur on vastly different time scales giving rise to prethermalization. Scattering processes involving two thermal phonons [see, e.g., Fig. 1(e)] eventually lead to a thermalization of the impurity. On shorter time scales, relevant to prepare and observe the prethermalized state, we find that one-phonon processes, which can only populate momentum states above a certain critical value, dominate over two-phonon processes. By contrast, two-phonon terms typically dominate the dynamics of two- and one-dimensional systems on all time scales, as we discuss elsewhere [28]. We note that while fast single-phonon scattering is forbidden for impurities with momenta below the Landau critical value by energy-momentum conservation, they can undergo higher-order scattering processes on very long time scales. For the emerging stationary momentum distribution in a one-dimensional Fermi gas see, e.g., [29].

Increasing the interaction strength between an impurity with sufficiently low momentum and the BEC leads to polaron dressing. While the polaronic binding energy is readily accessible by radio-frequency spectroscopy [30–32], other polaronic properties such as quasiparticle weight or effective mass must be deduced by other means. We show that the critical value $p_c^{(1)}$ for the final impurity is sensitive to small modifications of the impurity mass by phonon dressing. This could be used to measure the polaronic mass renormalization of an impurity at finite momentum.

*Corresponding author: mfleisch@physik.uni-kl.de

II. PRETHERMALIZED IMPURITIES IN ULTRACOLD BOSE-EINSTEIN CONDENSATES

A. Model

In the following we consider a single impurity atom (mass m_{I}) which is immersed in a BEC of a second bosonic species of atoms (mass m_{B}). We model their mutual interaction by a local contact potential with strength g_{IB}.

The atoms of the condensate are assumed to weakly interact with each other with interaction strength g. In this case the homogeneous BEC can be described using the Bogoliubov approximation, where the original boson operators $\hat{b}_{\boldsymbol{k}}$ are related to phonons $\hat{a}_{\boldsymbol{k}}$ by $\hat{b}_{\boldsymbol{k}} = \hat{a}_{\boldsymbol{k}} \cosh\theta_k - \hat{a}^\dagger_{-\boldsymbol{k}} \sinh\theta_k$ (see, e.g., [33]) and $\tanh^2\theta_k = (\frac{k^2}{2m_{\mathrm{B}}} + n_0 g - \omega_k)(\frac{k^2}{2m_{\mathrm{B}}} + n_0 g + \omega_k)^{-1}$. In this approximation the Hamiltonian of the BEC is just that of noninteracting phonons with momentum k,

$$\hat{\mathcal{H}}_0 = \int d^d k\, \omega_k \hat{a}^\dagger_{\boldsymbol{k}} \hat{a}_{\boldsymbol{k}}, \quad \omega_{\boldsymbol{k}} = ck(1 + k^2\xi^2/2)^{1/2}, \tag{1}$$

with $c = \sqrt{g n_0/m_{\mathrm{B}}}$ being the speed of sound and $\xi = 1/\sqrt{2 m_{\mathrm{B}} g n_0}$ the healing length of the BEC with density n_0. The interaction of a single impurity at position $\hat{\boldsymbol{r}}$ with the BEC reads

$$\hat{\mathcal{H}}_I = g_{\mathrm{IB}} \int d^d k \int d^d k' \hat{b}^\dagger_{\boldsymbol{k}} \hat{b}_{\boldsymbol{k}'} e^{i(\boldsymbol{k}-\boldsymbol{k}')\cdot\hat{\boldsymbol{r}}}. \tag{2}$$

Up to a constant energy offset this leads to the total Hamiltonian in d spatial dimensions

$$\begin{aligned}\hat{\mathcal{H}} = \epsilon_{\hat{\boldsymbol{p}}} &+ \int d^d k \left[\omega_k \hat{a}^\dagger_{\boldsymbol{k}} \hat{a}_{\boldsymbol{k}} + \frac{g_{\mathrm{IB}} n_0^{1/2}}{(2\pi)^{d/2}} W_k e^{i\boldsymbol{k}\cdot\hat{\boldsymbol{r}}} (\hat{a}^\dagger_{\boldsymbol{k}} + \hat{a}_{\boldsymbol{k}})\right] \\ &+ \frac{g_{\mathrm{IB}}}{2(2\pi)^d} \int d^d k \int d^d k' \big[\big(W_k W_{k'} + W_k^{-1} W_{k'}^{-1}\big) \hat{a}^\dagger_{\boldsymbol{k}} \hat{a}_{\boldsymbol{k}'} \\ &+ \tfrac{1}{2}\big(W_k W_{k'} - W_k^{-1} W_{k'}^{-1}\big)\big(\hat{a}^\dagger_{\boldsymbol{k}} \hat{a}^\dagger_{-\boldsymbol{k}'} + \hat{a}_{-\boldsymbol{k}} \hat{a}_{\boldsymbol{k}'}\big)\big] e^{i(\boldsymbol{k}-\boldsymbol{k}')\cdot\hat{\boldsymbol{r}}}.\end{aligned} \tag{3}$$

Here we consider trapped systems in $d = 3$ spatial dimensions, but will disregard the effects of the trapping potential to the Bogoliubov excitations. In addition, $\hat{\boldsymbol{p}}$ ($\hat{\boldsymbol{r}}$) are the impurity-momentum (position) operators and n_0 denotes the density of the condensate. Here and in the following we set $\hbar = 1$ and $k_B = 1$. Finally, we defined $W_k = [k^2\xi^2/(2 + k^2\xi^2)]^{1/4}$ and the kinetic energy of the impurity $\epsilon_{\hat{\boldsymbol{p}}} = \hat{\boldsymbol{p}}^2/2m_{\mathrm{I}}$.

The term in the first line of Eq. (3) corresponds to the Fröhlich Hamiltonian [34], known to describe polarons in solid-state systems. The Ginzburg radiation [35] resulting from the Fröhlich term has been investigated for particles with internal structure in [36]. The terms in the last two lines include two-phonon scattering terms, which in general need to be taken into account in a BEC [14,15,37].

B. Boltzmann equation

In the following we want to study the nonequilibrium dynamics of the Hamiltonian (3), starting from a BEC at finite temperature and a thermal momentum distribution of the impurity centered around a value $\boldsymbol{p}_0$. When their temperatures are given by T and T_{I}, respectively, the density matrix before the BEC-impurity interaction is $\hat{\rho}(0) = \exp[-(\hat{\boldsymbol{p}} - \boldsymbol{p}_0)^2/2m_{\mathrm{I}}T_{\mathrm{I}}] \otimes \exp[-\int d^d k\, \omega_k \hat{a}^\dagger_{\boldsymbol{k}} \hat{a}_{\boldsymbol{k}}/T]$. We consider the case when the temperature of the BEC is well below the critical temperature for condensation $T_{\mathrm{c}} = 2\pi n_0^{2/3}/m_{\mathrm{B}}\zeta(3/2)^{2/3}$, i.e., $T \ll T_{\mathrm{c}}$, and assume a heavy impurity, i.e., $m_{\mathrm{I}} > m_{\mathrm{B}}$.

We use a master equation to describe the dynamics of the impurity-density matrix $\hat{\rho}_{\mathrm{I}}(t)$, which can be derived by integrating out thermal phonons and employing the Born-Markov approximation. The Born approximation neglects higher-order scattering contributions and is valid for weak impurity-condensate interactions g_{IB}. This is equivalent to Fermi's golden rule with transition rates given by $\Gamma_{m\to n} = 2\pi\delta(E_m - E_n)|\langle n|\hat{\mathcal{H}}_I|m\rangle|^2$ [38]. In this way we obtain a linear Boltzmann equation for the momentum distribution $n_{\boldsymbol{p}}$ of the impurity, which has different contributions

$$\left.\frac{dn_{\boldsymbol{p}}}{dt}\right|_{\mathrm{sp,1ph}} = -\frac{g_{\mathrm{IB}}^2 n_0}{(2\pi)^{d-1}} \int d^d k\, W_k^2 [n_{\boldsymbol{p}} \delta(\epsilon_{\boldsymbol{p}} - \epsilon_{\boldsymbol{p}-\boldsymbol{k}} - \omega_k) - n_{\boldsymbol{p}+\boldsymbol{k}} \delta(\epsilon_{\boldsymbol{p}+\boldsymbol{k}} - \epsilon_{\boldsymbol{p}} - \omega_k)], \tag{4}$$

$$\left.\frac{dn_{\boldsymbol{p}}}{dt}\right|_{\mathrm{T,1ph}} = -\frac{g_{\mathrm{IB}}^2 n_0}{(2\pi)^{d-1}} \int d^d k\, \bar{n}_{\boldsymbol{k}}(T) W_k^2 (n_{\boldsymbol{p}} - n_{\boldsymbol{p}-\boldsymbol{k}}) [\delta(\epsilon_{\boldsymbol{p}} - \epsilon_{\boldsymbol{p}-\boldsymbol{k}} - \omega_k) + \delta(\epsilon_{\boldsymbol{p}-\boldsymbol{k}} - \epsilon_{\boldsymbol{p}} - \omega_k)], \tag{5}$$

$$\begin{aligned}\left.\frac{dn_{\boldsymbol{p}}}{dt}\right|_{\prec} = &-\frac{g_{\mathrm{IB}}^2}{8(2\pi)^{2d-1}} \int d^d k_1 d^d k_2 \big(W_{k_1} W_{k_2} - W_{k_1}^{-1} W_{k_2}^{-1}\big)^2 \{[1 + \bar{n}_{\boldsymbol{k}_1}(T)][1 + \bar{n}_{\boldsymbol{k}_2}(T)] \\ &\times [n_{\boldsymbol{p}} \delta(\epsilon_{\boldsymbol{p}} - \epsilon_{\boldsymbol{p}-\boldsymbol{k}_1-\boldsymbol{k}_2} - \omega_{k_1} - \omega_{k_2}) - n_{\boldsymbol{p}+\boldsymbol{k}_2+\boldsymbol{k}_1} \delta(\epsilon_{\boldsymbol{p}+\boldsymbol{k}_2+\boldsymbol{k}_1} - \epsilon_{\boldsymbol{p}} - \omega_{k_2} - \omega_{k_1})] + \bar{n}_{\boldsymbol{k}_1}(T) \\ &\times \bar{n}_{\boldsymbol{k}_2}(T) [n_{\boldsymbol{p}} \delta(\epsilon_{\boldsymbol{p}} + \omega_{k_1} + \omega_{k_2} - \epsilon_{\boldsymbol{p}+\boldsymbol{k}_1+\boldsymbol{k}_2}) - n_{\boldsymbol{p}-\boldsymbol{k}_2-\boldsymbol{k}_1} \delta(\epsilon_{\boldsymbol{p}} - \omega_{k_2} - \omega_{k_1} - \epsilon_{\boldsymbol{p}-\boldsymbol{k}_2-\boldsymbol{k}_1})]\},\end{aligned} \tag{6}$$

$$\begin{aligned}\left.\frac{dn_{\boldsymbol{p}}}{dt}\right|_{\times} = &-\frac{g_{\mathrm{IB}}^2}{4(2\pi)^{2d-1}} \int d^d k_1 d^d k_2 \big(W_{k_1} W_{k_2} + W_{k_1}^{-1} W_{k_2}^{-1}\big)^2 \bar{n}_{\boldsymbol{k}_1}(T) \big[\bar{n}_{\boldsymbol{k}_2}(T) + 1\big] \\ &\times \big[n_{\boldsymbol{p}} \delta\big(\epsilon_{\boldsymbol{p}} + \omega_{k_1} - \epsilon_{\boldsymbol{p}+\boldsymbol{k}_1-\boldsymbol{k}_2} - \omega_{k_2}\big) - n_{\boldsymbol{p}+\boldsymbol{k}_2-\boldsymbol{k}_1} \delta\big(\epsilon_{\boldsymbol{p}} + \omega_{k_2} - \epsilon_{\boldsymbol{p}+\boldsymbol{k}_2-\boldsymbol{k}_1} - \omega_{k_1}\big)\big].\end{aligned} \tag{7}$$

Here the thermal Bose-Einstein distribution function is given by $\bar{n}_{\boldsymbol{k}}(T) = [\exp(\omega_{\boldsymbol{k}}/k_{\mathrm{B}}T) - 1]^{-1}$.

The first two terms describe one-phonon emission, including spontaneous (sp) and thermally activated (T) processes. The third term ($\prec$) describes two-phonon creation or annihilation (thermal and spontaneous). These terms are illustrated in the diagrams shown in Figs. 1(c) and 1(d). The last term describes the scattering of a phonon at the impurity and is,

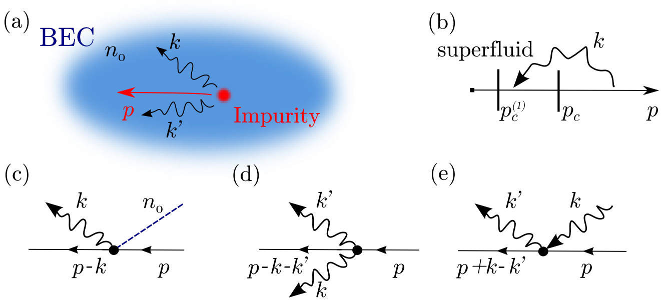

FIG. 1. (a) We consider impurity atoms inside an ultracold BEC of density n_0 in a thermal state. The emission of Cherenkov phonons of momentum k leads to dissipation of kinetic energy of the impurity with initial momentum p and thus to cooling. (b) Energy-momentum conservation permits single-phonon emission if the initial impurity momentum p is larger than the Landau critical value p_c and can lead to final momentum values above a critical value $p_c^{(1)}$, which is larger than zero if the impurity mass m_I is larger than the boson mass m_B. Also shown are elementary events corresponding to (c) single- and (d) two-phonon creation and (e) phonon scattering [see Eqs. (4)–(7)]. Two-phonon scattering depicted in (d) and (e) leads to corrections to the standard Fröhlich model.

in a weakly interacting BEC, where quantum depletion can be disregarded and in the lowest-order Born approximation in g_IB only relevant at finite temperatures. It is illustrated in Fig. 1(e). Due to the superfluidity of the BEC we expect that spontaneous phonon creation out of the condensate can only take place for impurity momenta p larger than the Landau critical momentum $p_\mathrm{c} = m_\mathrm{I} c$ and thus these processes cannot lead to a redistribution below p_c. Higher-order scattering will eventually lead to a thermalization of the impurity.

We have numerically simulated the time evolution of the momentum distribution of the impurity in a homogeneous BEC at finite $T \ll T_c$ using Eqs. (4)–(7). The results in Fig. 2 show the impurity momentum distribution $n_p = \int d^3\boldsymbol{p}' n_{\boldsymbol{p}'} \delta(p - |\boldsymbol{p}'|)$ of states having a momentum value of $|\boldsymbol{p}| = p$ with color encoded evolution time. One clearly recognizes that the emission of Cherenkov phonons leads to a fast population of momentum states below p_c but only above a certain critical momentum

$$p_\mathrm{c}^{(1)} = c\sqrt{m_\mathrm{I}^2 - m_\mathrm{B}^2}, \tag{8}$$

which can be derived from energy-momentum conservation associated with spontaneous single-phonon creation [see Eq. (B1)]. On a much longer time scale, two-phonon processes, not accounted for in the Fröhlich model, lead to a population of momentum states below $p_\mathrm{c}^{(1)}$. Here energy-momentum conservation leads to a second characteristic momentum scale for $T = 0$, provided $m_\mathrm{I} > 2m_\mathrm{B}$,

$$p_\mathrm{c}^{(2)} = c\sqrt{m_\mathrm{I}^2 - 4m_\mathrm{B}^2}. \tag{9}$$

One recognizes from Fig. 2 a clear separation of time scales for scattering events populating momenta above $p_\mathrm{c}^{(1)}$ versus those populating lower momenta. For $p_\mathrm{c}^{(2)}$ such a separation is much less visible however.

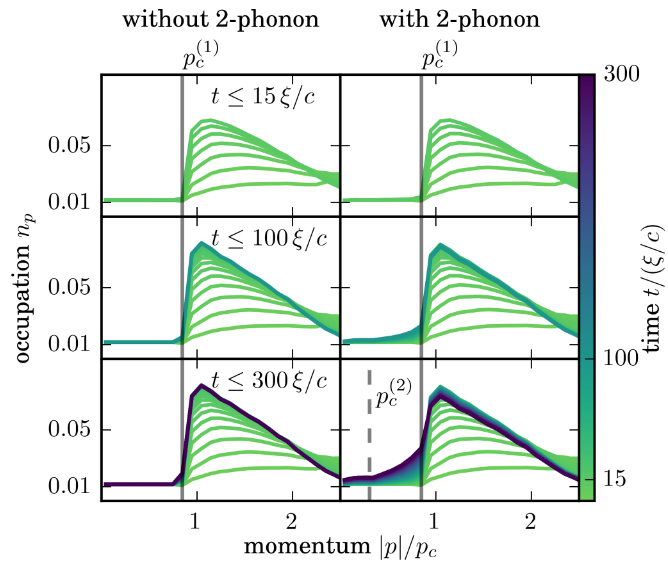

FIG. 2. Numerical simulation of the impurity momentum distribution when starting from a thermal state with $\boldsymbol{p}_0 = 0$ and $T_\mathrm{I} = 10T_\mathrm{c}$ and a low BEC temperature $T = 0.1T_\mathrm{c}$. Here we assume a peak density of $n_0 = 10/\xi^3$, $g_\mathrm{IB} = 1$, and a mass ratio $m_\mathrm{I}/m_\mathrm{B} = 87/39$ corresponding to a rubidium impurity in a potassium BEC. Momenta are given in units of the Landau critical momentum $p_\mathrm{c} = m_\mathrm{I} c$. The left column shows the dynamics including only single-phonon processes and the right column the dynamics including one- and two-phonon processes. Vertical lines indicate emerging critical momenta $p_\mathrm{c}^{(1)} = c\sqrt{m_\mathrm{I}^2 - m_\mathrm{B}^2}$ (solid vertical line) and $p_\mathrm{c}^{(2)} = c\sqrt{m_\mathrm{I}^2 - 4m_\mathrm{B}^2}$ (dashed vertical line).

From the Boltzmann equations one can determine the characteristic rates of spontaneous single-phonon ($\Gamma_\mathrm{1ph}^\mathrm{sp}$) and two-phonon ($\Gamma_\mathrm{2ph}^\mathrm{sp}$) processes for an initial impurity momentum p,

$$\Gamma_\mathrm{1ph}^\mathrm{sp}(p) = g_\mathrm{IB}^2 n_0 \int \frac{d^3k}{(2\pi)^2} W_k^2 \delta(\epsilon_{\boldsymbol{p}} - \epsilon_{\boldsymbol{p}-\boldsymbol{k}} - \omega_{\boldsymbol{k}}), \tag{10}$$

$$\Gamma_\mathrm{2ph}^\mathrm{sp}(p) = \frac{g_\mathrm{IB}^2}{2(2\pi)^5} \int d^3k \int d^3k' \left(\frac{W_k W_{k'} - W_k^{-1} W_{k'}^{-1}}{2} \right)^2 \times \delta(\epsilon_{\mathbf{p}} - \epsilon_{\boldsymbol{p}-\boldsymbol{k}-\boldsymbol{k}'} - \omega_{\boldsymbol{k}} - \omega_{\boldsymbol{k}'}). \tag{11}$$

The relative scaling of the two rates can be estimated as

$$\frac{\Gamma_\mathrm{2ph}^\mathrm{sp}}{\Gamma_\mathrm{1ph}^\mathrm{sp}} \sim \frac{1}{2\pi\xi^3 n_0}. \tag{12}$$

We have verified this scaling in our numerical simulations. For weak interactions $n_0\xi^3 \gg 1$ and thus spontaneous two-phonon scattering occurs at a much lower rate than single-phonon scattering, which leads to the separation of time scales observed in the numerical simulations.

C. Finite-temperature effects

Next we discuss the influence of a nonvanishing BEC temperature. While spontaneous scattering results in a fast increase of population in the momentum region $p_\mathrm{c}^{(1)} \leqslant p \leqslant p_\mathrm{c}$, thermal scattering can also cause a depopulation of that region. Thermally induced single-phonon scattering, however, cannot lead to impurity momenta below $p_\mathrm{c}^{(1)}$. Thus prethermalization

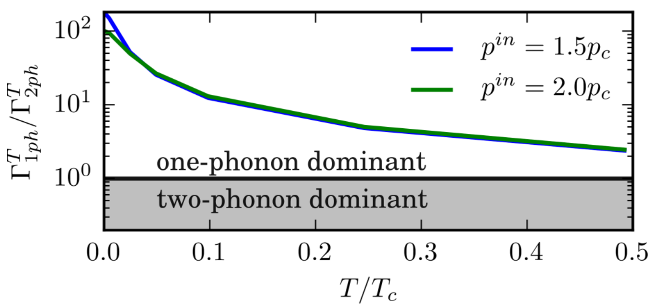

FIG. 3. Ratio of single-phonon to two-phonon scattering rates at finite T for different incoming impurity momenta. We find that scattering is dominated by single-phonon processes in either case, spontaneous ($T = 0$) or thermal. With an increasing BEC temperature, the two-phonon scattering rate increases faster than the single-phonon scattering rate, hence two-phonon processes become more important at large temperatures. Here $n_0 = 5$ and $\xi = 1$.

prevails also at finite T as long as single-phonon scattering dominates.

Since the two-phonon rate is proportional to the square of the thermal phonon number $\bar{n}_k^2$, it increases faster with temperature than the single-phonon rate. At a certain characteristic temperature $T_{\rm 2ph}$ there is a crossover between the single- and two-phonon-dominated regimes. This crossover can be characterized by considering the thermal phonon number at some characteristic phonon momentum $k_0 = 1/\xi \sim O(p_{\rm c})$. The thermal phonon number at $\boldsymbol{k}_0$ exceeds unity for $T > T_{\rm c}(n_0\xi^3)^{-2/3}$. Since for weak interactions $n_0\xi^3 \gg 1$, temperatures sufficiently below the critical temperature are required in order to be determined entirely by spontaneous processes. The crossover temperature $T_{\rm 2ph}$ can be estimated by setting the ratio of finite-T one- and two-phonon scattering rates $\Gamma^T_{\rm 2ph}/\Gamma^T_{\rm 1ph} \sim \bar{n}_{k_0}\Gamma^{\rm sp}_{\rm 2ph}/\Gamma^{\rm sp}_{\rm 1ph} = 1$. This yields

$$\left.\frac{T_{\rm 2ph}}{T_{\rm c}}\right|_{\rm 3D} \approx \frac{[\zeta(3/2)]^{2/3}}{\sqrt{2}}(n_0\xi^3)^{1/3}, \tag{13}$$

which, for weak interactions, is larger than unity and thus the crossover occurs only above $T_{\rm c}$. This is illustrated in Fig. 3, where we have plotted the ratio of rates of single- and two-phonon creation at finite temperature, obtained from numerical integration.

III. EFFECTS OF POLARONIC MASS RENORMALIZATION

While there is no spontaneous emission of Bogoliubov phonons for impurity momenta $p < p_{\rm c}$ (subsonic regime), the interaction with the condensate phonons leads to the formation of a polaron [34,39–41]. A polaron is a quasiparticle that describes the impurity dressed by a cloud of phonons carried along with the impurity. The strength of the impurity-BEC coupling is characterized by a dimensionless coupling constant α which describes the ratio of interaction energy to a characteristic energy scale of phonons [41]

$$\alpha = \frac{a_{\rm IB}^2}{a_{\rm BB}\,\xi}, \tag{14}$$

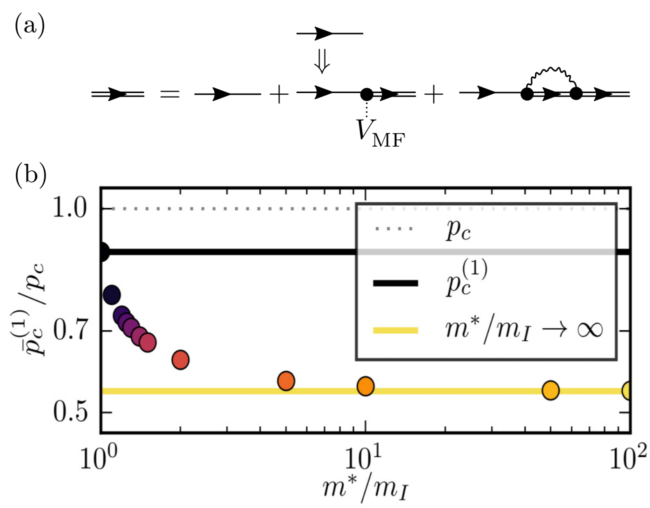

FIG. 4. (a) For weak interactions, polaron physics is well captured in the self-consistent Born approximation, which amounts to replacing the impurity propagator in Fig. 1(c) by a dressed propagator including mean-field $V_{\rm MF}$ and noncrossing phonon-exchange diagrams (see, e.g., [42]). (b) Effect of polaronic mass renormalization to cutoff momentum $p_{\rm c}^{(1)}$ of single-phonon scattering for mass ratio $m_{\rm I}/m_{\rm B} = 87/39$ corresponding to a Rb impurity in a K BEC. Instead of calculating polaronic effects explicitly, a phenomenological approach is used replacing the impurity mass $m_{\rm I}$ by a dressed mass m^* (see the text). The dressing $m^*/m_{\rm I}$ is color encoded. The black solid line depicts no dressing ($m^*/m_{\rm I} = 1$). The yellow solid line is a theoretical extrapolation showing that a finite critical momentum $p_{\rm c}^{(1)}$ exists even for heavy polarons ($m^*/m_{\rm I} \to \infty$).

where $a_{\rm IB}$ and $a_{\rm BB}$ are the impurity-boson and boson-boson scattering lengths and $g = 2\pi a_{\rm BB}/m_{\rm B}$ and $g_{\rm IB} = 2\pi a_{\rm IB}/m_{\rm red}$, with $m_{\rm red} = m_{\rm I}m_{\rm B}/(m_{\rm I} + m_{\rm B})$ being the reduced mass. In equilibrium the polaron energy and mass m^* are well defined quantities and can be calculated using different approaches [19,37,41]. In the regime of strong interactions these calculations are rather involved and some open questions remain, in particular under nonequilibrium conditions. For an impurity at rest and in lowest-order perturbation in the coupling strength α and at $T = 0$ one finds a linear dependence [41]

$$m^* - m_{\rm I} \sim \alpha. \tag{15}$$

In the following we argue that a measurement of the prethermalized momentum distribution of the impurity may offer an experimental approach to measure the polaronic mass renormalization.

The Hamiltonian (3) captures polaronic effects such as a mass renormalization. In the formal derivation of the scattering rates and the Boltzmann equations (4)–(7) one would have to replace the impurity propagator with a dressed propagator, as illustrated in Fig. 4(a) in self-consistent Born approximation, valid in the weak-interaction regime. This is, however, beyond the scope of our paper and we thus follow a purely phenomenological approach: In order to take into account the effects of a dressing of the impurity by phonons to the cooling dynamics, we replace the bare impurity propagator in the scattering diagrams of Fig. 1 by its free propagator for $p > m_{\rm I}c$ and by a dressed propagator for $p < m_{\rm I}c$, replacing the bare mass by (the unknown) dressed mass m^*,

$$\epsilon_p = \begin{cases} p^2/2m_\mathrm{I} & \text{if } p > p_\mathrm{c} \\ p^2/2m^* & \text{otherwise.} \end{cases} \tag{16}$$

Most interestingly, we find that the polaronic mass renormalization affects the cutoff momentum of the phonon scattering terms (8) and (9). Figure 4(b) shows the modified critical momentum $\overline{p_\mathrm{c}}^{(1)}$ for one-phonon scattering as a function of polaron mass (for details see Fig. 6 in Appendix C). One notices a sizable shift already for moderate mass renormalization. In the limit $m^*/m_\mathrm{I} \to \infty$ the cutoff approaches the value

$$\overline{p_\mathrm{c}}^{(1)} \longrightarrow p_\mathrm{c} - m_\mathrm{B} c \sqrt{\sqrt{4 + (m_\mathrm{I}/m_\mathrm{B})^2} - 2}. \tag{17}$$

IV. SUMMARY AND OUTLOOK

Concluding, we have numerically studied the cooling dynamics of individual impurities in a BEC at nonzero temperature, including scattering processes up to second order. We found that the range of accessible final impurity momenta is restricted to values above a critical momentum $p_c^{(1)}$ for short times, while equilibration to a thermal state occurs on a longer time scale, dominated by two-phonon scattering processes. This time-scale separation leads to a prethermalized quantum state of the impurity as long as energy redistribution by impurity-impurity interaction can be neglected.

Moreover, the critical momentum obtained depends on the mass renormalization of the polaronic quasiparticle state forming. This is an alternative route to experimentally measuring the polaronic mass shift in cold-atom experiments.

Importantly, our work paves the way for dynamical quantum state engineering of nonthermal impurity states, for example, by shaping its prethermalized momentum distribution. This can be done by operations selective on the impurity's momentum state being fast (slow) compared to the inverse two-phonon (one-phonon) rate.

ACKNOWLEDGMENTS

We thank K. Ünlütürk and H. Haug for valuable input at different stages of the work. A.W. and T.L. thank F. Grusdt for interesting and valuable input to the work. In addition, we thank Y. Shchadilova, D. Mayer, F. Kindermann, M. Hohmann, and F. Schmidt for stimulating discussions. T.L. acknowledges financial support from the Carl-Zeiss Stiftung. The work was supported by the Deutsche Forschungsgemeinschaft within the Sonderforschungsbereich TR49.

APPENDIX A: NUMERICAL MODELING

The simulations are performed by first evaluating the δ distribution in Eqs. (10) and (11) for a given incoming impurity moment $p^{(\mathrm{in})}$. Considering only one-phonon processes, this results in a large manifold of possible outgoing momenta $\{p^{(\mathrm{out})}\}$, forming a sharply defined 3D surface in momentum space (see Fig. 5 for illustration). Due to radial symmetry, these can be reduced in subsequent steps to eventually one dimension by radial integration, allowing for an efficient numerical calculation of scattering rates at moderate numerical effort. We thus obtain an evolution of the impurity state in momentum space, while in our approach the BEC remains a unperturbed quantum bath.

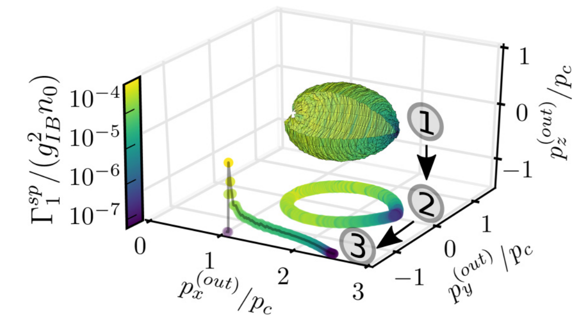

FIG. 5. Three-dimensional map of the spontaneous one-phonon scattering rate of different outgoing impurity momenta for an incoming impurity momentum of $\hat{\boldsymbol{p}}^{(\mathrm{in})} = 2.5 p_\mathrm{c}$. The numbers indicate the steps for dimensional reduction to one dimension, owing to the symmetry of scattering.

For two-phonon processes, the distribution of outgoing momenta is no longer restricted to the 3D surface in momentum space but becomes smeared out to a volume which is, however, sparsely filled. Clearly, in the limit of weak interactions $\xi^3 n_0 \gg 1$, the scattering rates for momenta in the inner (volume) part of the 3D momentum distribution are much smaller than the scattering rates corresponding to momenta on the surface; thus single-phonon scattering processes in the BEC lead to much faster dynamics than two-phonon scattering processes.

APPENDIX B: CRITICAL MOMENTA

All scattering processes in Eqs. (4)–(7) conserve both energy and momentum. When an incoming impurity momentum $p^{(\mathrm{in})}$ interacts with the bath and creates an excitation, the momentum k is transferred. The resulting momentum $p^{(\mathrm{out})}$ then fulfills

$$p^{(\mathrm{in})} - p^{(\mathrm{out})} - k = 0, \tag{B1}$$

$$\epsilon_{p^{(\mathrm{in})}} - \epsilon_{p^{(\mathrm{out})}} - \omega_k = 0. \tag{B2}$$

Obviously this limits the resulting impurity momenta in one dimension to

$$p^{(\mathrm{out})}(k) = \frac{m_\mathrm{I}}{k}(\omega_k - \epsilon_k). \tag{B3}$$

The resulting momentum $p^{(\mathrm{out})}$ has a global minimum when the created excitation and incoming impurity are antiparallel. Thus we obtain a global minimum for all dimensions $p^{(\mathrm{out})}_\mathrm{min}(k_c^{(1)}) = p_\mathrm{c}^{(1)}$ at $k_c^{(1)} = \frac{2c^2 m_\mathrm{I}^2}{p_c^{(1)}}$. This critical momentum $p_\mathrm{c}^{(1)} < p_\mathrm{c}$ [see Eq. (8)] exists for heavy impurities $m_\mathrm{I} > m_\mathrm{B}$ and is below the Landau critical momentum p_c. Given the case that the impurity is heavier $m_\mathrm{I} > 2m_\mathrm{B}$ than the boson mass, one finds a second critical momentum $p_\mathrm{c}^{(2)}$ for the spontaneous two-phonon scattering $\Gamma^{\mathrm{sp}}_{2\mathrm{ph}}$.

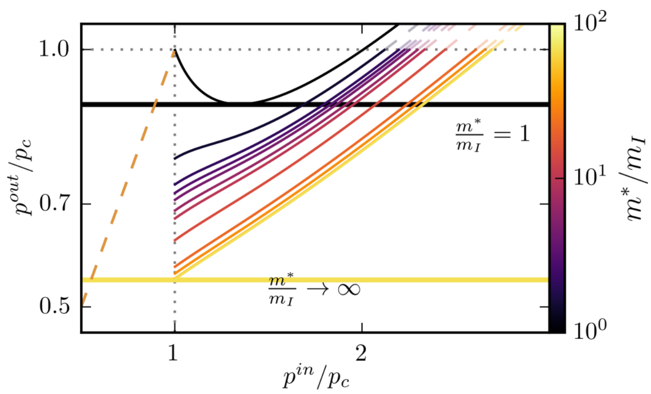

FIG. 6. Possible outgoing impurity momentum $p^{(\mathrm{out})}$ versus incoming impurity momentum $p^{(\mathrm{in})}$ for different effective impurity masses m^*/m_I. The bare impurity case (no dressing) is indicated by the black line, while an infinitely heavy polaron is indicated by the light yellow line. We find no solution of Eq. (B3) but the trivial $p^{\mathrm{in}} = p^{\mathrm{out}}$ if the impurity is already dressed by phonons $p^{(\mathrm{in})}/p_\mathrm{c} \leqslant 1$ (dashed orange line). We define the minimum of $p^{(\mathrm{out})}$ for every dressing curve as the first critical momentum $p_\mathrm{c}^{(1)}$ for this dressing. These minima are plotted versus the respective mass ratio in Fig. 4(c).

APPENDIX C: POLARONIC MASS RENORMALIZATION

The polaronic dressing of the impurity leads to changes of the impurity's interaction with the quantum gas. First, modifications of the energy spectrum due to the polaronic binding energy have been measured in the vicinity of a Feshbach resonance [20,21]. Second, the effective mass of the impurity is expected to change due to polaron formation. For our system we thus expect a modification of the critical momentum that an impurity may reach via the resonant scattering processes depicted in Fig. 1. We introduce the polaron mass m^* and effectively replace the free impurity propagator by a free polaron particle if the impurity's velocity becomes smaller than the speed of sound c. When applying this to Eqs. (4)–(7) the integral kernels remain untouched, though the energy conservation is affected, leading to a change of new critical momenta, which are a result of Eqs. (B1) and (B2). Inserting the dispersion relation (16) into momentum- and energy-conservation relations [see Eq. (B3)], we find a decrease of the critical momentum $p_\mathrm{c}^{(1)}$ with increasing dressing (see Fig. 6). The minima here are below $p_\mathrm{c}^{(1)}$ and therefore redefine the critical momentum. These minima are plotted versus the respective mass ratio in Fig. 4(c).

[1] A. J. Leggett, Bose-Einstein condensation in the alkali gases: Some fundamental concepts, Rev. Mod. Phys. **73**, 307 (2001).
[2] J. Weiner, V. S. Bagnato, S. Zilio, and P. S. Julienne, Experiments and theory in cold and ultracold collisions, Rev. Mod. Phys. **71**, 1 (1999).
[3] L. Pitaevskii and S. Stringarii, *Bose-Einstein Condensation and Superfluidity* (Oxford University Press, New York, 2016), p. 576.
[4] T. Kinoshita, T. Wenger, and D. S. Weiss, A quantum Newton's cradle, Nature (London) **440**, 900 (2006).
[5] S. Hofferberth, I. Lesanovsky, B. Fischer, T. Schumm, and J. Schmiedmayer, Non-equilibrium coherence dynamics in one-dimensional Bose gases, Nature (London) **449**, 324 (2007).
[6] M. Rigol, V. Dunjko, and M. Olshanii, Thermalization and its mechanism for generic isolated quantum systems, Nature (London) **452**, 854 (2008).
[7] J. Berges, S. Borsányi, and C. Wetterich, Prethermalization, Phys. Rev. Lett. **93**, 142002 (2004).
[8] M. Gring, M. Kuhnert, T. Langen, T. Kitagawa, B. Rauer, M. Schreitl, I. Mazets, D. A. Smith, E. Demler, and J. Schmiedmayer, Relaxation and prethermalization in an isolated quantum system, Science **337**, 1318 (2012).
[9] A. C. Hewson, *The Kondo Problem to Heavy Fermions* (Cambridge University Press, Cambridge, 1997), p. 444.
[10] A. V. Gorshkov, M. Hermele, V. Gurarie, C. Xu, P. S. Julienne, J. Ye, P. Zoller, E. Demler, M. D. Lukin, and A. M. Rey, Two-orbital SU(N) magnetism with ultracold alkaline-earth atoms, Nat. Phys. **6**, 289 (2010).
[11] F. Chevy and C. Mora, Ultra-cold polarized Fermi gases, Rep. Prog. Phys. **73**, 112401 (2010).
[12] R. Olf, F. Fang, G. E. Marti, A. MacRae, and D. M. Stamper-Kurn, Thermometry and cooling of a Bose gas to 0.02 times the condensation temperature, Nat. Phys. **11**, 720 (2015).
[13] L. Mathey, D.-W. Wang, W. Hofstetter, M. D. Lukin, and E. Demler, Luttinger Liquid of Polarons in One-Dimensional Boson-Fermion Mixtures, Phys. Rev. Lett. **93**, 120404 (2004).
[14] S. P. Rath and R. Schmidt, Field-theoretical study of the Bose polaron, Phys. Rev. A **88**, 053632 (2013).
[15] W. Li and S. Das Sarma, Variational study of polarons in Bose-Einstein condensates, Phys. Rev. A **90**, 013618 (2014).
[16] J. Levinsen, M. M. Parish, and G. M. Bruun, Impurity in a Bose-Einstein Condensate and the Efimov Effect, Phys. Rev. Lett. **115**, 125302 (2015).
[17] L. A. Peña Ardila and S. Giorgini, Impurity in a Bose-Einstein condensate: Study of the attractive and repulsive branch using quantum Monte Carlo methods, Phys. Rev. A **92**, 033612 (2015).
[18] L. A. Peña Ardila and S. Giorgini, Bose polaron problem: Effect of mass imbalance on binding energy, Phys. Rev. A **94**, 063640 (2016).
[19] Y. E. Shchadilova, F. Grusdt, A. N. Rubtsov, and E. Demler, Polaronic mass renormalization of impurities in Bose-Einstein condensates: Correlated Gaussian-wave-function approach, Phys. Rev. A **93**, 043606 (2016).
[20] M. G. Hu, M. J. Van de Graaff, D. Kedar, J. P. Corson, E. A. Cornell, and D. S. Jin, Bose Polarons in the Strongly Interacting Regime, Phys. Rev. Lett. **117**, 055301 (2016).
[21] N. B. Jørgensen, L. Wacker, K. T. Skalmstang, M. M. Parish, J. Levinsen, R. S. Christensen, G. M. Bruun, and J. J. Arlt, Observation of Attractive and Repulsive Polarons in a Bose-Einstein Condensate, Phys. Rev. Lett. **117**, 055302 (2016).
[22] A. J. Daley, P. O. Fedichev, and P. Zoller, Single-atom cooling by superfluid immersion: A nondestructive method for qubits, Phys. Rev. A **69**, 022306 (2004).
[23] A. Griessner, A. J. Daley, S. R. Clark, D. Jaksch, and P. Zoller, Dark-State Cooling of Atoms by Superfluid Immersion, Phys. Rev. Lett. **97**, 220403 (2006).
[24] A. Griessner, A. J. Daley, S. R. Clark, D. Jaksch, and P. Zoller, Dissipative dynamics of atomic Hubbard models coupled to a phonon bath: Dark state cooling of atoms within a Bloch band of an optical lattice, New J. Phys. **9**, 44 (2007).

[25] R. Scelle, T. Rentrop, A. Trautmann, T. Schuster, and M. K. Oberthaler, Motional Coherence of Fermions Immersed in a Bose Gas, Phys. Rev. Lett. **111**, 070401 (2013).
[26] D. Chen, C. Meldgin, and B. DeMarco, Bath-induced band decay of a Hubbard lattice gas, Phys. Rev. A **90**, 013602 (2014).
[27] M. Hohmann, F. Kindermann, T. Lausch, D. Mayer, F. Schmidt, E. Lutz, and A. Widera, Individual Tracer Atoms in an Ultracold Dilute Gas, Phys. Rev. Lett. **118**, 263401 (2017).
[28] T. Lausch, A. Widera, and M. Fleischhauer, Role of higher-order phonon scattering for impurity cooling in a low-dimensional BEC, arXiv:1712.07912.
[29] O. Gamayun, O. Lychkovskiy, E. Burovski, M. Malcomson, V. V. Cheianov, and M. B. Zvonarev, Quench-controlled frictionless motion of an impurity in a quantum medium, arXiv:1708.07665.
[30] M. Koschorreck, D. Pertot, E. Vogt, B. Fröhlich, M. Feld, and M. Köhl, Attractive and repulsive Fermi polarons in two dimensions, Nature (London) **485**, 619 (2012).
[31] R. Schmidt and T. Enss, Excitation spectra and rf response near the polaron-to-molecule transition from the functional renormalization group, Phys. Rev. A **83**, 063620 (2011).
[32] A. Shashi, F. Grusdt, D. A. Abanin, and E. Demler, Radio-frequency spectroscopy of polarons in ultracold Bose gases, Phys. Rev. A **89**, 053617 (2014).
[33] C. J. Pethick and H. Smith, *Bose-Einstein Condensation in Dilute Gases* (Cambridge University Press, New York, 2008).
[34] H. Fröhlich, Electrons in lattice fields, Adv. Phys. **3**, 325 (1954).
[35] V. L. Ginzburg, Radiation by uniformly moving sources, Phys. Usp. **39**, 973 (1996).
[36] J. Marino, A. Recati, and I. Carusotto, Casimir Forces and Quantum Friction from Ginzburg Radiation in Atomic Bose-Einstein Condensates, Phys. Rev. Lett. **118**, 045301 (2017).
[37] R. S. Christensen, J. Levinsen, and G. M. Bruun, Quasiparticle Properties of a Mobile Impurity in a Bose-Einstein Condensate, Phys. Rev. Lett. **115**, 160401 (2015).
[38] A derivation of the quantum mechanical generalization of the Boltzmann equation can be found, e.g., in the following textbooks: W. Greiner, *Quantum Mechanics: Special Chapters* (Springer, Berlin, 1998), Chap. 4; F. Schwabl, *Statistical Mechanics* (Springer, Berlin, 2006), Chap. 11.
[39] L. D. Landau and S. I. Pekar, Effective mass of a polaron, Zh. Eksp. Teor. Fiz. **18**, 419 (1948).
[40] F. M. Cucchietti and E. Timmermans, Strong-Coupling Polarons in Dilute Gas Bose-Einstein Condensates, Phys. Rev. Lett. **96**, 210401 (2006).
[41] J. Tempere, W. Casteels, M. K. Oberthaler, S. Knoop, E. Timmermans, and J. T. Devreese, Feynman path-integral treatment of the BEC-impurity polaron, Phys. Rev. B **80**, 184504 (2009).
[42] F. Grusdt and E. Demler, New theoretical approaches to Bose polarons, arXiv:1510.04934.